INFLUENCES FROM ONE SI-INTEGRATED SUBJACENT SHEET UPON OPTIC ATTRIBUTES IN INGAN/GAN QUANTUM WELL FORMATIONS FEATURING DISPARATE QUANTITIES FOR QUANTUM WELL UNITS

Le Thi Trang[1], *Dang Truong Thinh*[2], *Ha Thanh Tung* [3,*]

[1]Faculty of Information Technology, Dong Nai Technology University, Dong Nai Province, Vietnam.
[2]Faculty of Electrical and Electronics Engineering, Ton Duc Thang University, Ho Chi Minh City, Vietnam.
[3]Faculty of Basic Sciences, Vinh Long University of Technology Education, Vinh Long Province, Vietnam

*Corresponding Author: Ha Thanh Tung (Email: tunght@vlute.edu.vn)
(Received: 14-May-2025; accepted: 23-September-2025; published: 30-September-2025)
http://dx.doi.org/10.55579/jaec.202593.496

Abstract. *The study herein concerns the optic attributes for multiple InGaN polar quantum well formations featuring disparate quantities for quantum well units (QWU) developed using one InGaN Si-integrated subjacent sheet. With a small quantity for QWUs, it is possible overshadow the ambient-heat inner quantum proficiency via thermal-ion discharge generated by QWUs. Said mechanism may manifest as the radioactive reconsolidation pace within InGaN QWUs may become small, caused by the integrated electrical zone throughout QWUs that assist the thermal-ion discharge activity in maintaining presence proficiently under ambient heat that impedes the intrinsic quantum proficiency. For the formations in our study, the radioactive reconsolidation pace would escalate under the influences from the Si-integrated subjacent sheet that abates the electrical zone throughout the QWUs. Under said mechanism, the influence from thermal-ion discharge would be substantially abolished, and as such, the inner quantum proficiency under ambient heat would not be related to the QWU quantity.*

Keywords: *White LED; Lambert-Beer law; Color rendering index; Luminous efficacy; Quantum specks.*

1. Introduction

Multiple earlier works have examined the influences from introducing sheets developed before the initial QWU within InGaN/GaN (I/G) illuminating diode units (LEDs) as well as formations under photoluminescent (PL) testing [1–3]. Said sheets, called subjacent sheets (SS), would be typically sheets for n-integrated InGaN featuring small In amounts [4–6]. According to past works, the sheets' presence may

yield many augmentations such as greater PL as well as electroluminescent (EL) intenseness under small as well as ambient heat along with greater inner quantum proficiency (IQP). On the other hand, the reasons behind said augmentations are not fully explained [7]. According to several works, the unpremeditated polarizing process for category III-nitride matters causes diminution zones with a contrary nature based on the standards of the zones throughout the QWUs induced via piezoelectrical processes [8]. Moreover, the Fermi state affixation induced via n-category integration may prove useful for regulating the potency for said zone near the exterior for one GaN formation, influencing the discharge attributes for QWUs developed within said zone via alterations for the quantum restricted Stark activity (QRSA). Based on some speculations, as a result, the proficiency augmentations perceived within formations featuring SS would be caused by the boosted electron-cavity ripple factor that results in a greater radioactive reconsolidation pace posterior to one decline for the electric zone throughout the QWUs [9–11]. Said mechanism would typically manifest under the stronger presence against the nonradioactive activities related to faults from adulterations. On the other hand, introducing SS into formations abates adulteration integration upon interact points, resembling the earliest data concerning GaAs/AlGaAs (G/A) formations [12–14].

The advantages for IQP in QWU formations were examined when it comes to abating the proficiency for nonradioactive trails connected to faults as well as adulterations but not influences connected to the form in QWU formations. Judging established knowledge, it is possible to substantially altered the ambient-heat IQP for QWU formations via altering the QWU quantity. Specifically, the thermal-ion for conveyors within QWUs may become a proficiency-impeding activity for singular G/A QWU formations as well as singular I/G QWUs. It is possible to circumvent said mechanism within multi-quantum well (MQW) formations via reseizing the optically roused conveyors through remaining QWUs within aggregations. The study herein aims at validating if it is possible to circumvent the influences from thermal-ion discharge via introducing SS capable of abating radioactive reconsolidation pace, achieving a degree where it is possible to mitigate the thermic-based exclusion for blockades [15–17].

2. Experimental

Our I/G QWU sampling units featuring SS were developed via the metallic-organic fume accumulation (MOFA) in our study that utilizes the dual-heat (DH) developing approach. The units were developed above one GaN quasi-substrate substances upon sapphire. In the case of every unit, one GaN:Si frame was developed, preceding one InGaN:Si SS featuring an identical integrating denseness to said frame. Above the SS, one unintegrated GaN sheet was developed preceding the QWUs as well as blockades. The quantity for QWU-blockade durations saw variance. The QWU breadths, In portions as well as blockade thicknesses were identified via Xray diffraction assessments via one Philips X' Pert setting. As InGaN is utilized in this case, the emitted wavelength can range between UV and green in the spectrum. On the other hand, the DH developing approach causes significant well breadth variances. As such, one version for the first Xray diffraction utilized in the study of Vickers' team was employed. With one $\omega - 2\theta$ scanning process for the symmetrical 002 reflectivity, Xray diffraction may precisely identify the breadth for one QWU-blockade pair as well as the median In portion across the whole QWU-blockade pair. The distinctive assessment for the QWU breadth, In portion as well as blockade breadth is decided by the manifestation for one absent satellite apex for said scanning process. On the other hand, said absent apex did not manifest as QWUs display considerable variances for breadth. For the task of acquiring the QWU breadth as well as constitution, two extra five-QWU units were developed via the identical developing criteria with one difference of the GaN blockade being altered. Through the assessment for the QWU-blockade breadth for our units, one functioning QWU breadth, being the median breadth for QWUs, as well as the matching functioning QWU constitution

were subject to extrapolation. Our granular stress microscopic (GSM) assessments exhibited a lack of consistent variance for the denseness in V trenches upon the exteriors from our units [18–20].

The optic attributes were assessed via the merger between continual ripple PL spectroscopic assessment as well as PL degradation duration assessment. Our units were positioned above the chill tip of one heat-regulated closed-sequence He cryogenic apparatus. In the case of the temporal degradation assessments, our units underwent excitation via the periodicity threefold output for one Ti:sapphire laser. The continual ripple PL spectroscopic assessment was carried out through regulating the illumination via one He/Cd laser or one diode laser featuring one cleaver as well as through scattering the PL utilizing one singular latticework spectrometric apparatus tracked via one optic-multiplying pipe. The indicator generated by said optic-multiplying apparatus was assessed via one lock-in tracker. In the case of the PL temporal-degradation assessments, one microscopic pathway disk tracker was employed for tracking the PL through said spectrometric apparatus while the indicator was assessed via the temporal-associated singular photonic quantifying approach [21–23].

3. Results and Discussion

Judging the recreated conductivity bar as well as valent bar data in the case of our units assessed via the Nextnano setting, the In portion would be identical regarding every QWU within every formation. The location pivot would be identified via the positive developing pathway reaching the unit exterior in which null value would be fixed upon the interact point among the SS as well as nadir QWU blockade. The power pivot would be identified via the Fermi extent under null value. According to the work of Davies' team, the Fermi extent would be affixed unto the conductivity bar rim within the SS zone as well as unto the valent bar rim upon the unit exterior with the substance being unintegrated. The potency for the yielded exterior diminution zone, matching the general incline among said locations, abates under surging QWU quantity. The electrical zones throughout one QWU in every unit were assessed via the recreated bar rim data [24].

The electrical zone in the case of the singular-QWU unit would be negative, denoting that the unit assumes a reverse pathway unlike the remaining units. The median electrical zone throughout the QWUs surges under the escalating QWU quantity. Regarding every QWU within every unit featuring at least two QWU, excluding the initial QWU from the units featuring ten as well as fifteen QWUs, the electrical zone potency shows little variance among the QWUs within one specific unit. In the case of the excluded units mentioned, the electrical zone throughout the initial QWU within the aggregation would be abated, correlating with the second QWU. Said mechanism results from the extra film charge manifesting upon the I/G interact point among the SS as well as the initial QWU blockade caused by the significant polarizing inconsistency among the dual sheets, exhibiting a contrary nature based on the standards of the film charge generated upon the I/G interact point upon the nadir for the initial QWU within the aggregation. The In presence within the singular-QWU unit would be substantially tinier judging the standard of the remaining units. The abated In portions for the singular-QWU unit suggests an abated influence through the stress-generated piezoelectrical zone, accompanied by the yielded zone abatement activity generated via the exterior diminution zone. Regardless, the SS plays a significant role in altering the yielded electrical zone among the singular- as well as triple-QWU units [25].

SiO_2 is useful when combined with optic phosphor samples in WLED devices because to its unique optical qualities, which include a high refractivity index and strong dispersion capabilities. SiO_2 granules, when combined with phosphor sheets, have the capacity to alter the interaction between light and substances. SiO_2 may be used as effective small dispersers capable of guiding and scattering light emitted by LED chips, resulting in improved illumination dispersion and more uniform lighting allocation. By adjusting the SiO_2 dosage in combination with other phosphor samples, optical parameters like as chromatic rendition, CCT, and bright-

ness may be regulated consistently. Aside from dispersion, SiO_2 may increase chroma rendition when used with common phosphor samples like YAG:Ce.

Figure 1 below features the changes of the scattering coefficients under different wavelengths. It is well known that the scattering coefficient may evaluate optical performance in WLED devices by boosting dispersion activities, which improves chroma and illumination allocation precision. In any event, significant concentrations of that material may impair brightness because light is limited or directed inefficiently. Said coefficient steadily decreases from its peak as wavelength increases, which causes dispersion for the light produced by the blue chip to propagate and then more convert into rays at longer wavelengths [26]. These changes appear to be the result of an inverse mechanism. Then, when the blue-ray dispersion in the front discharge surge with the blue-ray repeating absorptivity and rear-dispersion decreased, the luminescence will be increased [27–29]. When the particle size increases, the YAG:Ce content must decrease in order to achieve this goal, which is demonstrated by Figure 2 exhibiting the YAG:Ce content being influenced by the particle size. As can be seen, the content considerably falls as the particle size escalates. The particle size also affects CCT levels, as shown by Figure 3. Under a particle size of 19 wt.%, the CCT shows the most noticeable fluctuations. The CCT is at its lowest under particle size of 17 and 19 wt.%. In contrast, the CCT reaches its peak under the particle size of 19 wt.% [30]. The hue aberration shows inconsistent fluctuations under various particle sizes, as demonstrated by Figure 4. Notably, the hue aberration shows a very significant increase when the particle size reaches 15 wt.%, then considerably abates at 17 wt.%. The aberration manages to show a moderate surge as the particle size rises further before plummeting again at 21 wt.%. For the lumen in LED shown in Figure 5, it displays an inverse correlation with the particle size, consistently declining as the particle size becomes greater. The observed changes may be the consequence of the difference in color allocation and the lower intensity of the blue discharge due to increased rear-dispersion and repeated absorptivity. It should be noted that as particle

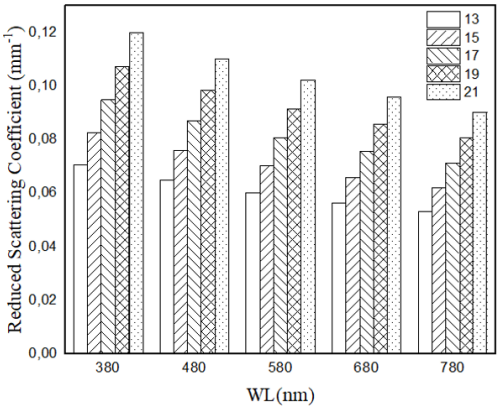

Fig. 1: Relationship between scattering coefficient and wavelength.

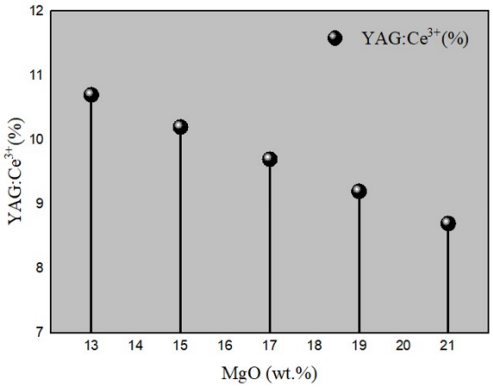

Fig. 2: YAG:Ce presence interacting with particle size of SiO_2.

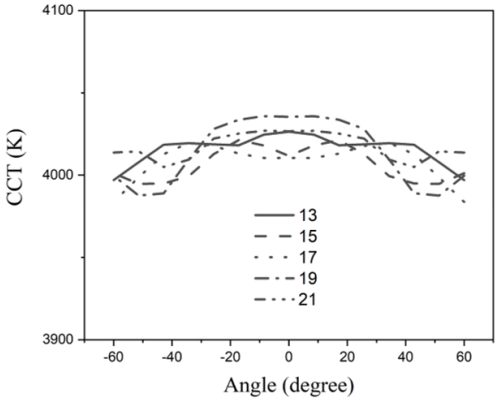

Fig. 3: CCT alteration based on particle size.

size increases, the phosphor sheet typically has a wider width, which lowers the energy of the whole spectrum. As a result, the lighting trans-

mutation between blue and yellow or red-orange will be more pronounced. This indicates that the transmuted beam may participate in rear-reflection under extremely large particle sizes, which would reduce the luminous intensity and produce a higher CCT level. The particle size

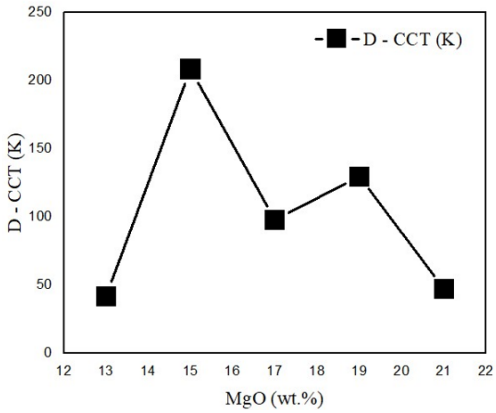

Fig. 4: Variation in hue aberration under SiO_2 particle size.

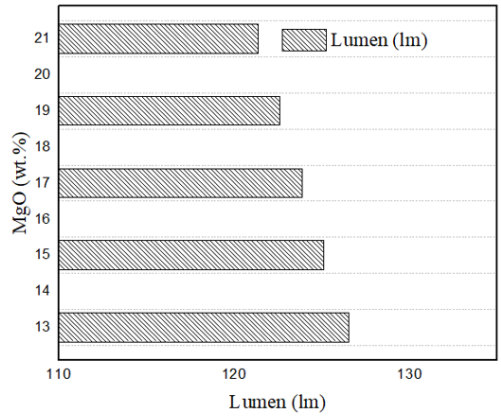

Fig. 5: LED lumen generated based on SiO_2 particle size.

has an impact on the WLED device's color generation output as well. In Figure 6, there are small declines for CRI as the particle size grows from 13 to 21 wt.%. Regarding the CQS in Figure 7, it manages to show a moderate boost under 15 wt.%, but is ultimately subject to declining like CRI, albeit to a much more considerable extent. The color difference between the orange-yellow, blue, and green components may be the cause of several crashes that have been seen. The reason for this discrepancy is that with large particle sizes, the increased dispersion produces more orange-yellow components since the discharge color of the rays often favors the orange-yellow zone. Therefore, excessive dispersion may result in lower CRI and CQS.

Concerning the task of measuring hue quality, CRI would be considered the most common and the oldest index. In order to gauge hue quality, CRI assesses eight hue samples under testing illumination and natural illumination, then compares the conditions. CRI proves to be useful when it comes to assessing hue performance in illumination with wide spectrum. However, this index was developed well before the development of LED devices, and thus, is not suitable to apply on these devices. Using only the few hue samples from CRI, the desaturation resulted would be too much for appropriately assess chromatic output from LED devices. CQS was proposed to remedy this weakness, by assessing fifteen hue samples, and thus is capable of yielding more authentic hue assessments. In addition to increased hue samples, CQS also include other factors: individual's taste and hue disparity. As a newer index proposed in a modern era, CQS would be a more fitting index for examining the hue performance in modern devices like LED.

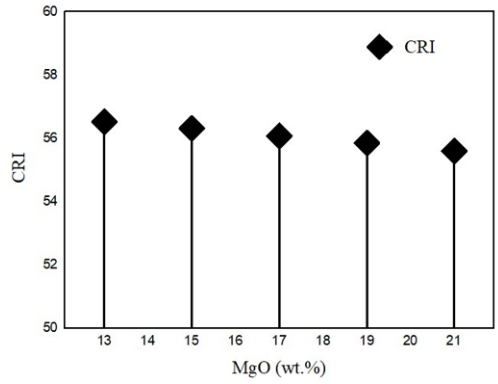

Fig. 6: CRI subject to changes in SiO_2 particle size.

4. Conclusion

The influences from the thermal-ion under ambient heat were mitigated via the SS introduced

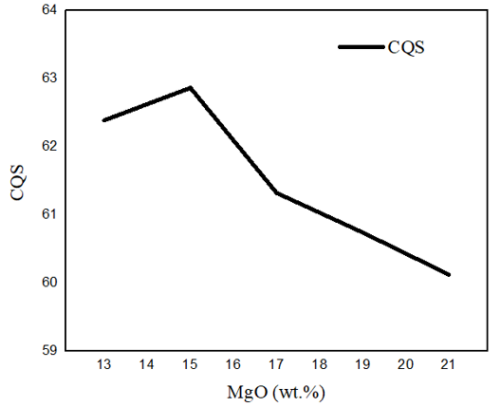

Fig. 7: CQS under influence of SiO_2 particle size.

into our sampling units as the IQPs for the singular- as well as triple-QWU formations would surpass the remaining units. Meanwhile, in case the thermal-ion discharge became prevalent, these factors would be smaller. Said mechanism results from the abatement for the QRSA while the resulting surge for the radioactive pace would be adequate for circumventing the influences from thermal-ion discharge. Regarding the remaining units, the alteration for radioactive pace would be particularly faint while the IQP displays a visible decline under the surging well quantity. With our assessments carried out under one continual exciting energy denseness, the conveyor denseness, the conveyor denseness for each QWU abates when the well quantity surges within the disparate units, and as a result, potentially enabling nonradioactive reconsolidation upon faults as well as adulterations for attaining greater proficiency under declining conveyor denseness within our units.

References

[1] H. T. Tung, B. T. Minh, N. L. Thai, H. Y. Lee, and N. D. Q. Anh. Zno particles as scattering centers to optimize color production and lumen efficiencies of warm white leds. *Optoelectron. Adv. Mater. - Rapid Commun.*, 18(5–6):1–6, Jun 2024.

[2] P. H. Cong, L. X. Thuy, N. T. P. Loan, H. Y. Lee, and N. D. Q. Anh. Zno-doped yellow phosphor compound for enhancing phosphor-conversion layer's performance in white leds. *Optoelectron. Adv. Mater. - Rapid Commun.*, 18(7-8):389–395, Jul-Aug 2024.

[3] P. X. Le, N. D. Q. Anh, and H. Y. Lee. Regulating the white led properties with different sio2 particle sizes. *Optoelectron. Adv. Mater. - Rapid Commun.*, 18(9-10):485–489, Sep-Oct 2024.

[4] N. D. Q. Anh and H. Y. Lee. Titanium dioxide in vanadate red phosphor compound for conventional white light emitting diodes. *Optoelectron. Adv. Mater. - Rapid Commun.*, 18(9-10):480–484, Sep-Oct 2024.

[5] P. H. Cong and N. D. Q. Anh. Augmenting chroma performance for wled employing sr8znsc(po4)7:eu2+@sio2 as a scattering-enhancing substance. *Sci. Technol. Indonesia*, 10(2):467–472, Mar 2025.

[6] N. D. Q. Anh, N. T. P. Loan, P. V. De, and H. Y. Lee. Potassium bromide scattering simulation for improving phosphor-converting white led performance. *Optoelectron. Adv. Mater. - Rapid Commun.*, 19(7-8):378–383, Jul-Aug 2025.

[7] Y. Peng, H. Cheng, Z. Chen, M. Chen, and H. Wang. Luminous efficacy enhancement of phosphor-in-glass based white light-emitting diodes through patterned structure. In *2016 17th International Conference on Electronic Packaging Technology (ICEPT)*, pages 65–68, Wuhan, China, 2016.

[8] D. M. Kim, B. J. Shin, H. S. Tae, and J. H. Seo. Improvement of luminous efficacy using short sustain pulsewidth and long off-time between sustain pulses in ac plasma display panel. *IEEE Trans. on Plasma Sci.*, 41(4):887–891, Apr 2013.

[9] G. He and J. Tang. Spectral optimization of phosphor-coated white leds for color rendering and luminous efficacy. *IEEE Photonics Technol. Lett.*, 26(14):1450–1453, Jul 2014.

[10] J. H. Mun, S. H. Kim, and K. C. Choi. Ac microplasma device with a cylindrical hollow electrode for improving luminous efficacy. *IEEE Trans. on Electron Devices*, 56(9):1930–1934, Sep 2009.

[11] Z. Liu, W. B. Hu, and C. L. Liu. Luminance and luminous efficacy improvement of mercury-free flat fluorescent lamp with arclike electrode. *IEEE Trans. on Plasma Sci.*, 38(10):2860–2866, Oct 2010.

[12] N. Somchaiwong and E. Chaidee. Comparison of power quality and luminous efficacy of commercial energy saving lamps in thailand. In *2012 12th International Conference on Control, Automation and Systems*, pages 1800–1804, Jeju, Korea (South), 2012.

[13] M. E. Raypah, B. K. Sodipo, M. Devarajan, and F. Sulaiman. Estimation of luminous flux and luminous efficacy of low-power smd led as a function of injection current and ambient temperature. *IEEE Trans. on Electron Devices*, 63(7):2790–2795, Jul 2016.

[14] Y. J. Saw, V. Kalavally, and C. P. Tan. The spectral optimization of a commercializable multi-channel led panel with circadian impact. *IEEE Access*, 8:136498–136511, 2020.

[15] X. Yu, B. Xie, Q. Chen, Y. Ma, R. Wu, and X. Luo. Thermal remote phosphor coating for phosphor-converted white-light-emitting diodes. *IEEE Trans. on Components, Packag. Manuf. Technol.*, 5(9):1253–1257, Sep 2015.

[16] M. Balsky and T. Terrich. Light trespass in street led lighting systems. In *2020 21st International Scientific Conference on Electric Power Engineering (EPE)*, pages 1–4, Prague, Czech Republic, 2020.

[17] Z. Cai et al. Enhancing optical performance for white light-emitting diodes using quantum- dots/boron nitride hybrid reflective structure. *IEEE Trans. on Electron Devices*, 69(10):5580–5589, Oct 2022.

[18] W. Yang et al. Photometric optimization of color temperature tunable quantum dots converted white leds for excellent color rendition. *IEEE Photonics J.*, 8(5):1–11, Oct 2016.

[19] H. Xiao et al. Improvements on remote diffuser-phosphor-packaged light-emitting diode systems. *IEEE Photonics J.*, 6(2):1–8, Apr 2014.

[20] T. Shinoda and K. Awamoto. Plasma display technologies for large area screen and cost reduction. *IEEE Trans. on Plasma Sci.*, 34(2):279–286, Apr 2006.

[21] S. H. Kim, J. H. Mun, and K. C. Choi. Study on the discharge modes of the microplasma generated in a plasma display with an auxiliary electrode. *IEEE Trans. on Plasma Sci.*, 37(2):327–333, Feb 2009.

[22] F. Xie, W. Zeng, Z. Hu, G. Yang, and B. Yu. High-quality white laser diode fabricated by laser-driven tricolor pig film-on-sapphire. *IEEE Trans. on Electron Devices*, 69(9):4987–4991, Sep 2022.

[23] H. V. Demir. Quality led lighting and displays using nanocrystals. In *2013 IEEE Photonics Conference*, pages 19–19, Bellevue, WA, USA, 2013.

[24] Q. Meng, H. Rao, Q. Zhang, K. Zhang, W. Zheng, and T. Li. Optimized self-adaptive phosphor coating structure of white leds by conventional dispensing method. *IEEE Trans. on Components, Packag. Manuf. Technol.*, 7(12):1965–1968, Dec 2017.

[25] H. T. Tung, N. T. P. Loan, and N. D. Q. Anh. The enhancement chromatic uniformity and illuminating flux of wleds with dual-layer phosphorus configuration. In *Lecture Notes in Electrical Engineering*, pages 167–174. Springer, 2024.

[26] V. T. Pham, N. H. Phan, G.-F. Luo, H.-Y. Lee, and D. Q. A. Nguyen. The application of calcium carbonate caco3 and titania tio2 for color homogeneity and luminous flux enhancement in pc-leds. *J. Adv. Eng. Comput.*, 5(2):75, Jun 2021.

[27] N. H. S. Dang, D. M. T. Nguyen, T. P. L. Nguyen, D. Q. A. Nguyen, and H.-Y. Lee. Enhance wleds performance with additional phosphor materials in multi-layer remote structure. *J. Adv. Eng. Comput.*, 5(3):167, Sep 2021.

[28] N. D. M. Thong, D. N. H. Son, S. D. Ho, N. D. Q. Anh, and H.-Y. Lee. The use of y3al5o12:ce3+ and catio3:pr3+ in a dual-layer remote phosphor configuration improves the optical efficiencies of a phosphor-in-glass white light-emitting diode. *J. Adv. Eng. Comput.*, 6(1):36, Mar 2022.

[29] H. Saito, H. Hatanaka, and M. Nakajima. Motion image reconstruction of luminous intensity distribution of plasma using light emission computed tomography. In *Proceedings of the 1992 International Conference on Industrial Electronics, Control, Instrumentation, and Automation*, volume 3, pages 1608–1612, San Diego, CA, USA, 1992.

[30] H. T. Tung, N. T. P. Loan, and N. D. Q. Anh. The enhancement chromatic uniformity and illuminating flux of wleds with dual-layer phosphorus configuration. In *Lecture Notes in Electrical Engineering*, pages 167–174. Springer, 2024.

About Authors

Le Thi TRANG received a Master's degree in Information Technology from Lac Hong University, Vietnam, and is currently working as a lecturer at the Faculty of Information Technology, Dong Nai Technology University, Bien Hoa City, Vietnam. Her research interests include computer science, computer vision, image recognition and classification, face detection and recognition, abnormal motion detection, and graphic design. She can be contacted at email: lethitrang@dntu.edu.vn.

Dang Truong THINH was born in Can Tho city, Vietnam. He has been studying at the Faculty of Electrical and Electronics Engineering, Ton Duc Thang University. His research interest is optoelectronics. He can be reached via email: 42100128@student.tdtu.edu.vn.

Ha Thanh TUNG received the Ph.D degree in physics from University of Science, Vietnam National University Ho Chi Minh City, Vietnam, he is working as a lecturer at the Faculty of Basic Sciences, Vinh Long University of Technology Education, Vietnam. His research interests focus on developing the patterned substrate with micro- and nano-scale to apply for physical and chemical devices such as solar cells, OLED, and photoanode. He can be contacted at email: tunght@vlute.edu.vn.